Int. J. Heat Mass Transfer. Vol. 25, No. 3, pp. 325 335, 1982
Printed in Great Britain

0017-9310/82/030325-11 $03.00/0
Pergamon Press Ltd.

A NUMERICAL MODEL FOR TURBULENT NON-EQUILIBRIUM DISPERSED FLOW HEAT TRANSFER

STEPHEN W. WEBB* and JOHN C. CHEN†

(*Received* 6 *February* 1981 *and in revised form* 5 *August* 1981)

Abstract—An analytical model has been developed for the prediction of two-phase turbulent, non-equilibrium, dispersed flow heat transfer in post-CHF flow boiling. The thermodynamic non-equilibrium is treated through a vapor generation source function in the vapor conservation equations to represent the heat sink/mass source effect of the droplet evaporation. Effects of various components in the model are evaluated. A limited data–model comparison shows average deviations of -7.9% and $+6.6\%$ for predicted vapor and wall superheats with respect to measured values.

NOMENCLATURE

a, vapor generation source function variable;
C_d, drag coefficient;
C_p, specific heat;
d, droplet diameter;
D, pipe diameter;
g, gravitational constant;
i, enthalpy;
k, conductivity;
l, mixing length;
P, pressure;
Pr, Prandtl number;
q'', heat flux;
r, radial direction;
R, pipe radius;
Re, Reynolds number;
S, slip ratio;
t, temperature;
V, velocity;
x, quality;
y, distance from wall $= R - r$;
z, axial direction.

Greek symbols

α, vapor void fraction;
Γ, vapor generation source function;
ε, eddy diffusivity;
μ, viscosity;
ρ, density;
τ, shear stress.

Subscripts

c, convection;
CHF, critical heat flux;
d, droplet;
f, fluid;
g, gas;
h, heat;
l, liquid, laminar;
m, momentum;
r, radial, radiation;
R, relative;
s, saturation;
t, turbulent, total;
v, vapor;
w, wall;
z, axial.

* Applied Engineering Analysis Dept., Gilbert Associates, Inc., Reading, PA 19603, U.S.A.
† Institute of Thermo-Fluid Engineering & Science, Lehigh University, Bethlehem, PA 18015, U.S.A.

INTRODUCTION

PREDICTION of two-phase heat transfer for post-CHF (critical heat flux) conditions in flow boiling is important in the analysis of the reflooding phase of postulated nuclear reactor accidents. Heat transfer in this mode is significantly less efficient then nucleate boiling heat transfer since liquid phase contact at the wall becomes unstable. The vapor and entrained liquid droplets can be in thermodynamic non-equilibrium with superheated vapor, as first suggested by experiments performed by Parker and Grosh [1]. An analytical model for dispersed flow heat transfer must accurately predict the superheated wall and vapor temperatures in the presence of droplets.

PREVIOUS WORK

Many models for post-CHF heat transfer in flow boiling have been proposed. The models can be classified as empirical or phenomenological. In general, the empirical models fit the data to a proposed relationship while the phenomenological models take into account the physical processes involved. Phenomenological models can be further subdivided into models which use existing heat transfer correlations and those that solve the conservation equations. A number of previous models are summarized in Table 1 according to the classifications discussed above.

Those models using the conservation equation approach will be discussed briefly. Sun *et al.* [2] proposed the first post-CHF heat transfer model based on the conservation equations. The fully developed vapor energy equation for laminar flow, including the effects of radiation, was solved with the droplets modelled as distributed heat sinks. Axial variation of

Table 1. Classification of post-CHF heat transfer models

Empirical	Phenomenological	
	Existing correlations	Conservation equations
Slaughterbeck, Vesely, Ybarrondo, Condie, and Mattson [42]	Laverty and Rohsenow [45]	Sun, Gonzalez-Santalo and Tien [2]
Tong and Young [43]	Forslund and Rohsenow [46]	Dix and Andersen [3]
Groeneveld [10]	Hynek, Rohsenow and Bergles [47]	Yao [4]
Groeneveld and Delorme [44]	Iloeje, Plummer, Rohsenow and Griffith [48]	Rane and Yao [5]
	Plummer, Griffith and Rohsenow [49]	Yao and Rane [6, 9]
	Chen, Sundaram and Ozkaynak [50]	Wong [7]
	Ganic and Rohsenow [51]	Wong and Hochreiter [8]
	Jones and Zuber [52]	
	Saha, Shiralkar and Dix [53]	

the vapor temperature was assumed negligible. Dix and Anderson [3] used 1-dim. conservation equations for the liquid and the vapor, including interfacial effects. The convective heat transfer coefficient derived by Sun *et al.* was used to evaluate the wall temperatures. Subsequent laminar flow models by Yao [4–6] and Wong [7, 8] used the basic approach of Sun *et al.* with axial temperature variation. Wong analyzed a rod bundle geometry while Yao simplified the model by considering constant fluid properties and neglecting radiation heat transfer. Yao and Rane [9] extended the above analyses for turbulent flow. All of the above analyses modelled the heat sink term by specifying the droplet size and vapor–droplet heat transfer coefficient.

Since thermodynamic non-equilibrium may exist, wall and vapor temperatures should be measured and used to evaluate the predictive capability of any model. The only model to use the conservation equations and measured wall and vapor temperatures is that of Wong [7, 8]. However, the model was only verified for laminar flow conditions. No other turbulent flow model has been compared with measured vapor and wall temperature data, as is necessary to ascertain the accuracy of the model.

PRESENT MODEL

The flow pattern associated with post-CHF heat transfer is a function of the quality or void fraction at which CHF occurs. At low or subcooled qualities, the pattern is inverse annular flow which consists of a central liquid core surrounded by an annular vapor film. Higher qualities lead to a dispersed flow pattern which is a vapor continuum with entrained liquid droplets. A dispersed flow pattern will eventually develop even if the flow pattern is initially inverse annular. According to Groeneveld [10], the dispersed flow pattern is encountered at void fractions in excess of 80%. Figure 1 shows the flow pattern, wall superheat, and quality variation for this high void fraction case. The present model is concerned with a dispersed flow pattern.

Post-CHF heat transfer in non-equilibrium dispersed flow can be described by the general two-phase conservation equations for the vapor and liquid phases. The conservation equations used in the present model include a vapor generation source term to represent the heat sink effect of the evaporating droplets, instead of a detailed droplet model. This form of the conservation equations is similar to the formulations in the RELAP 5 [11] and TRAC [12] computer codes. These advanced reactor safety codes recognize the importance of non-equilibrium but do not yet have reliable models for post-CHF flow boiling conditions. Hopefully, the results from this investigation can be used directly in these reactor safety codes to improve their theoretical basis.

CONSERVATION EQUATIONS

The general set of six conservation equations is too complicated to be solved without a large number of simplifications (see Ishii [13]). Considering radial geometry in a pipe with upward vertical flow, the simplifications used in the present model are:

1. Steady state conditions
2. Axial symmetry
3. Negligible direct wall to liquid heat transfer
4. Radially uniform droplet distribution
5. Uniform heating of vapor due to radiation heat transfer
6. Negligible viscous dissipation
7. Saturation conditions for liquid droplets.

The key of the present approach is to solve the vapor conservation equations and include liquid vaporization effects through the vapor source function.

The heat transfer mechanisms in the present model are depicted in Fig. 2. Convection and radiation heat transfer are considered as is the associated mass transfer. Direct heat transfer from the wall to the droplets is neglected since liquid phase contact with the wall is unstable at the wall temperatures encountered.

The other assumptions are straightforward. Quasi-steady state conditions are applicable to the reflood situation in a reactor as demonstrated by Arrieta and Yadigaroglu [14] and Ghazanfari *et al.* [15]. A radially uniform droplet distribution is supported by Cumo [16] for dispersed flow and Lee and Durst [17]

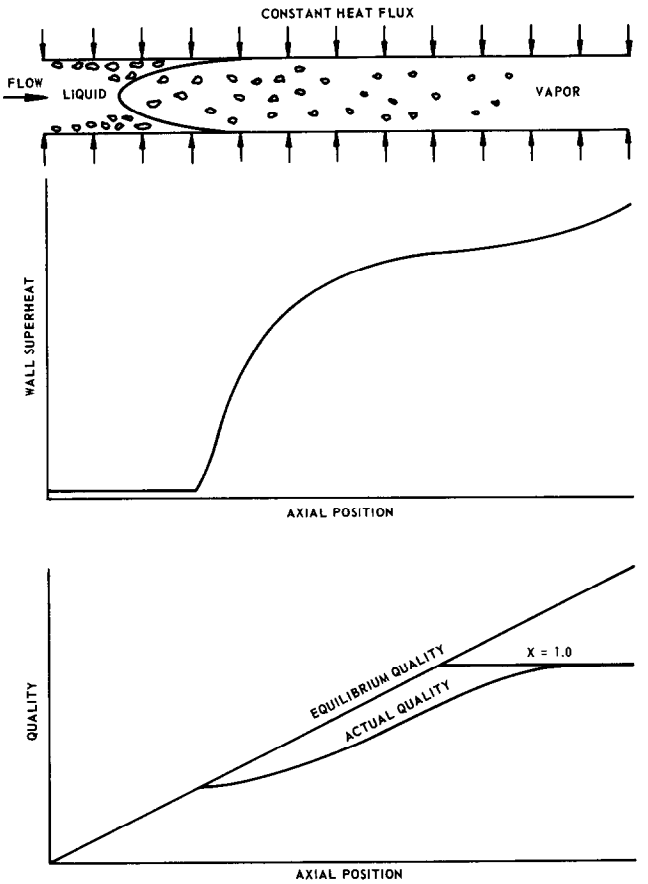

FIG. 1. Typical dispersed flow conditions.

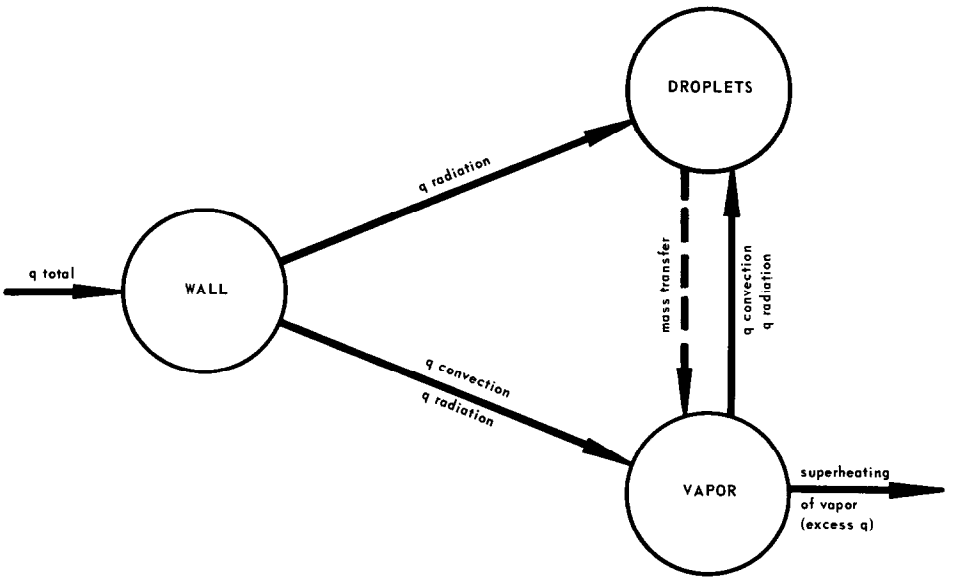

FIG. 2. Heat transfer mechanisms in the present model.

for turbulent particle flow. The assumption of uniform radiation to vapor is reasonable for optically-thin vapor. Interfacial forces and the relative velocity terms in the momentum equations are negligible at the low mass fluxes encountered in reflood situations. Slip is considered however in estimating the void fraction.

Using the above simplifications, the vapor conservation equations become:

Continuity

$$\frac{\alpha}{r}\frac{\partial}{\partial r}(r\rho_v V_r) + \frac{\partial}{\partial z}(\alpha\rho_v V_z) = \Gamma_t; \quad (1)$$

Momentum

$$-\frac{dP}{dz} = \rho_v V_r \frac{\partial V_z}{\partial r} + \rho_v V_z \frac{\partial V_z}{\partial z} - \frac{1}{r}\frac{\partial}{\partial r}\left(r\mu_v \frac{\partial V_z}{\partial r}\right) + \rho_v g; \quad (2)$$

Energy

$$\rho_v c_{pv}\left[V_r \frac{\partial t_v}{\partial r} + V_z \frac{\partial t_v}{\partial z}\right] = \frac{\Gamma_r}{\alpha}(i_{vs} - i_v) + \frac{\Gamma_c}{\alpha}(i_{ls} - i_v) + \frac{4}{\alpha D}(q''_{r,w-v} - q''_{r,v-d}) + \frac{1}{r}\frac{\partial}{\partial r}\left(rk_v \frac{\partial t_v}{\partial r}\right). \quad (3)$$

The equation set is closed by the conservation of mass requirement. The above equations have the following initial and boundary conditions:

$$t_v(z=0) = t_s,\ V_z(z=0) \rightarrow \text{fully developed}; \quad (4a)$$

$$\frac{\partial t_v}{\partial r}(r=R) = -\frac{q''_{w,c}}{k_v} = -\frac{q''_t - q''_{r,w-v} - q''_{r,w-d}}{k_v};$$

$$\frac{\partial t_v}{\partial r}(r=0) = 0. \quad (4b)$$

$$V_z(r=R) = 0, \quad \frac{\partial V_z}{\partial r}(r=0) = 0; \quad (4c)$$

$$V_r(r=R) = 0, \quad V_r(r=0) = 0. \quad (4d)$$

CONSTITUTIVE RELATIONSHIPS

In order to solve the above set of equations, various constitutive relationships are needed. The various thermodynamic properties are taken from the 1967 ASME Steam Tables [18]. The vapor generation source function, radiation heat transfer, void fraction, and turbulent viscosity and conductivity relationships are discussed in this section in detail.

The vapor generation source function represents the heat sink/mass source effect of the phase change of the water droplets. Convection and radiation components are included, so the source function is

$$\Gamma_t = \Gamma_c + \Gamma_r. \quad (5)$$

The convection source function, Γ_c, has usually been related in other studies to the droplet size and a given heat transfer correlation as discussed earlier. The present model lumps all these parameters into a variable which may be correlated through operating conditions. The present convection source function is dependent only upon the local vapor superheat and a measure of the droplet surface area for a constant number of drops, or

$$\Gamma_c = a(t_v - t_s)(1-\alpha)^{2/3}, \quad (6)$$

where the value of a is varied for each run in order to match the experimental data.

This specific form of the vapor generation source function does not include specification of the droplet size or the vapor-to-droplet heat transfer coefficient. These parameters are difficult to measure in actual film boiling conditions and are basically unknown at this time. The present formulation in terms of a lumped vapor generation source function, a, is suggested as a pragmatic approach to circumvent these unknowns. The hope is that experimental non-equilibrium vapor superheat data can be used to correlate a as a function of system and operating conditions.

The radiation portion of the vapor generation source function is due to heat transfer to the droplets by radiation. The radiation source function is assumed to be constant in the radial direction in order to apply the simplified radiation heat transfer model. The resulting radiation source function for a circular tube is:

$$\Gamma_r = \frac{4}{D}(q''_{r,w-d} + q''_{r,v-d})/(i_{vs} - i_{ls}). \quad (7)$$

The total vapor generation source function becomes

$$\Gamma_t = a(t_v - t_s)(1-\alpha)^{2/3} + \frac{4}{D}(q''_{r,w-d} + q''_{r,v-d})/(i_{vs} - i_{ls}). \quad (8)$$

Radiation heat transfer among the wall, vapor, and droplets is based on the work of Sun *et al.* The model assumes an optically thin vapor–droplet mixture resulting in a simple three node network analysis. This optically thin assumption is generally met under the conditions of interest. The necessary vapor absorption coefficient is derived from a curve fit to the data of Abu-Romia and Tien [19] as given by Wong [7]. The model necessitates specification of a droplet size which also effects the void fraction model which will be discussed. For the present analysis, an initial droplet diameter of 0.000762 m (0.03 inches) is used consistent with the results of Wong. The number of droplets is assumed constant, so the droplet size is a function of axial location. The dependence of the overall results upon this assumed droplet size will be discussed later.

The void fraction is calculated by equating the drag force on a droplet to the sum of the gravitational and

buoyancy forces for upward vertical flow. The resulting equations are:

$$\alpha = \left(1 + \frac{(1-x)}{x}\frac{\rho_g}{\rho_f} S\right)^{-1}, \tag{9}$$

$$S = \frac{V_g}{V_g - V_R}, \tag{10}$$

$$V_R = \left[\frac{4}{3}\frac{d}{C_d}\left(\frac{\rho_f}{\rho_g} - 1\right)\right]^{1/2}, \tag{11}$$

$$C_d = \frac{24}{Re_d} + \frac{6}{1 + Re_d^{1/2}} + 0.4. \tag{12}$$

The drag coefficient equation is from White [20]. Average velocities and densities have been used to simplify the resulting equations.

The viscosity and conductivity values used in the conservation equations include laminar and turbulent contributions, or:

$$\mu_v = \mu_{v,l} + \mu_{v,t}, \tag{13}$$

$$k_v = k_{v,l} + k_{v,t}. \tag{14}$$

The laminar values are thermodynamic properties of the vapor phase while the turbulent portion is a function of local flow quantities.

Due to the large vapor void fractions for the conditions of the data (~99%), single phase theory for the vapor phase has been used. Prandtl's mixing length theory is used to evaluate the turbulent viscosity, or:

$$\mu_{v,t} = \frac{\tau_t}{\partial V_z/\partial y} = \rho_v l^2 \frac{\partial V_z}{\partial y}. \tag{15}$$

The Prandtl mixing length theory as given above assumes a constant density for the momentum exchange of the turbulent fluid. In the present case, and in most heat transfer situations, the fluid density varies in the y direction. Mixing length theory has been modified to account for this fact, so

$$\mu_{v,t} = l^2 \frac{\partial}{\partial y}(\rho_v V_z), \tag{16}$$

which, for constant density flow, reduces to the expression given earlier.

The modified Prandtl mixing length theory has been used by Pai [21] for the turbulent jet mixing of two gases, Hsu and Smith [22] to determine the density variation effect on critical region heat transfer, and Levy [23] for two-phase flow. In the present case, the vapor density variation in the y direction is considered since the vapor momentum equation is being solved.

The mixing length evaluation follows the general procedure of Na and Habib [24]. The Nikuradse (25) mixing length expression for pipe flow is combined with the Van Driest [26] damping factor, so

$$\frac{l}{R} = \left[0.14 - 0.08\left(1 - \frac{y}{R}\right)^2 - 0.06\left(1 - \frac{y}{R}\right)^4\right] \times [1 - \exp(-y^+/A^+)] \tag{17}$$

where A^+ is equal to 26.

For the turbulent eddy conductivity, a turbulent Prandtl number approach was used. The definition of a turbulent Prandtl number is

$$Pr_t = \frac{\varepsilon_m}{\varepsilon_h}. \tag{18}$$

Using the definitions of the eddy diffusivities

$$Pr_t = \frac{\mu_{v,t} C_{pv}}{k_{v,t}}. \tag{19}$$

A study of turbulent Prandtl number models for air in wall-bounded shear flow has been conducted by Webb [27]. The Azer and Chao [28] model is appropriate for pipe flow ($dp/dz < 0$), and their expression for fluids with Prandtl numbers between 0.6 and 15 is

$$Pr_t = \frac{1 + 57\, Re^{-0.46}\, Pr^{-0.58} \exp\left[-\left(\frac{y}{R}\right)^{1/4}\right]}{1 + 135\, Re^{-0.45} \exp\left[-\left(\frac{y}{R}\right)^{1/4}\right]} \tag{20}$$

SOLUTION TECHNIQUE

The momentum and energy equations are parabolic partial differential equations which are solved by the Keller Box Method [29], which allows for continually variable mesh point spacing in the solution. The resulting equations can be manipulated, as discussed by Ackerberg and Phillips [30], to form a tridiagonal matrix for temperature and velocity which are solved by a direct elimination algorithm [31]. Iteration is necessary to arrive at a prescribed heat flux. A slight modification of the equations is necessary at the tube centerline as is usual for cylindrical geometry cases.

Verification of the solution method for a fully developed velocity profile has been made by comparison to analytical solutions for laminar and turbulent flows. These solutions include heat sources in their formulation which can easily be modified for heat sinks by changing the appropriate sign; no mass transfer is considered in these models. For laminar flow, the results match the Nusselt numbers of Sparrow and Siegel [32] within 0.4%. The turbulent predictions match the Siegel and Sparrow [33, 34] results within 10%. By changing the eddy diffusivity models in the present model to those used by Siegel and Sparrow, the differences are improved to approx. 1%, well within the accuracy of the analytical results provided.

RESULTS AND DISCUSSION

Wall and vapor temperatures are necessary for a comprehensive model evaluation. Unfortunately, superheated vapor temperature measurements with entrained droplets in post-CHF flow are extremely difficult, and only a few attempts have been reported. Mueller [35] and Polomik [36] obtained a limited

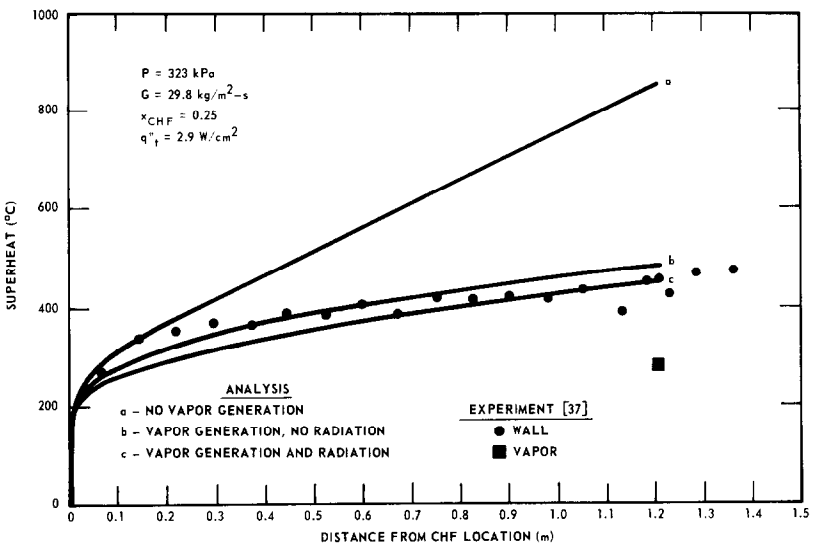

FIG. 3. Effect of vapor generation and radiation on wall superheat (low quality).

number of values at high qualities in a tube. Hochreiter [37] measured vapor temperatures in rod bundles, also at high quality. Recently, Nijhawan *et al.* [38, 39] obtained measurements at low pressures in a tube for a wide range of qualities. A total of over 200 data points were collected. The parametric trends observed in the experiments are given by Nijhawan *et al.* [40]. The data of Nijhawan are the best documented results to date and were used exclusively in the model evaluation.

The conditions of Nijhawan's experiments indicate a dispersed flow pattern for all but a few of his data points, according to the criterion of Groeneveld. The two experimental runs chosen for comparison are for low and moderate qualities. The strength of the vapor generation source function was varied to match the experimental vapor temperature to the calculated bulk vapor temperature. The predicted wall temperatures are then compared to the measured data. The influence of the various components in the model is discussed below.

Vapor generation

Curves a and b in Figs. 3 and 4 show the wall

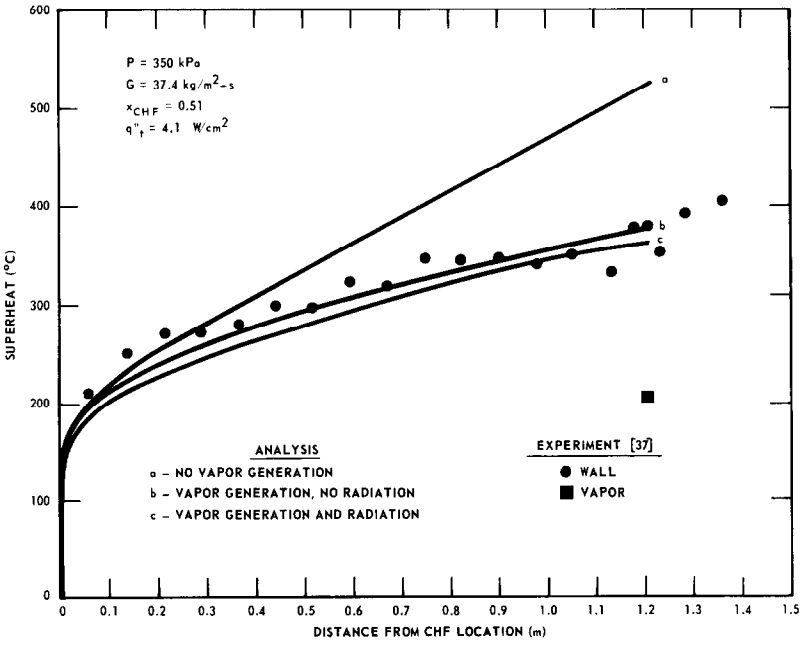

FIG. 4. Effect of vapor generation and radiation on wall superheat (medium quality).

superheats with and without vapor generation. Without vapor generation, which is a frozen quality model, the vapor temperature cannot be matched, and the wall superheat is significantly overpredicted. These wall superheats are reduced approx. 300–350°C at the vapor temperature measurement location by the addition of sufficient vapor generation to match the measured vapor temperature. An equilibrium post-CHF heat transfer model is also in poor agreement with the data as shown by Webb and Chen [41]. Therefore, the correct amount of vapor generation is important and must be included in any post-CHF heat transfer model.

Form of Γ_c

The form of the vapor generation source function is not important for the present data. A radially and axially uniform convection source function does almost as well as the model given by equation (6). However, inclusion of the local vapor superheat and droplet surface area parameter should be important in correlating the source function with other experimental data.

Radiation heat transfer

The wall superheat with vapor generation is given by curve b in Figs. 3 and 4. Curve c in these figures includes the addition of radiation heat transfer to the model. The calculated wall superheats are reduced about 30°C by the addition of this heat transfer component. Approximately 10–20% of the total heat flux is transferred from the wall to the two-phase fluid by radiation.

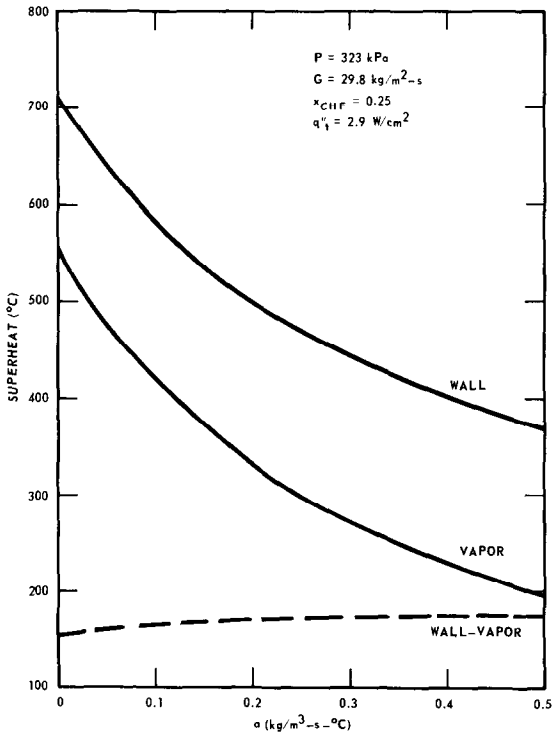

FIG. 5. Effect of vapor generation source strength on superheat temperatures (low quality).

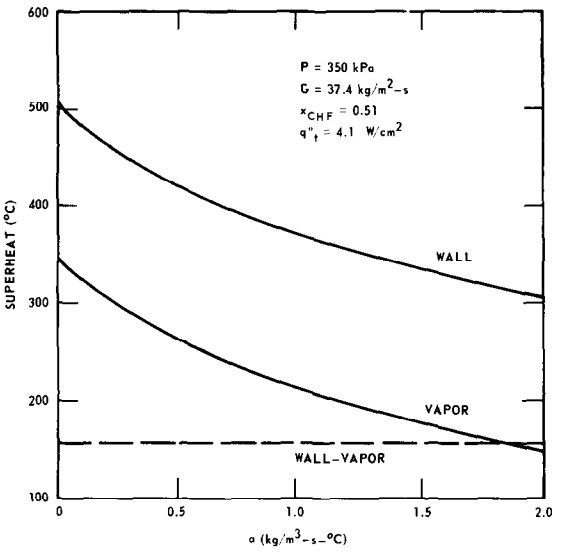

FIG. 6. Effect of vapor generation source strength on superheat temperatures (medium quality).

Momentum equation

The general conservation equations include a radial vapor velocity to include the effects of a developing axial velocity profile for the vapor. Since the vapor generation is most intense near the wall, where local vapor velocities are lowest, the velocity profile is continually developing. However, if the radial vapor velocity is calculated and used in the conservation equations, the wall superheats are reduced slightly for the first 0.1–0.2 m downstream of CHF. Differences further downstream are negligible. Therefore, a fully developed vapor velocity profile can be used in the analysis. All the results shown in this paper are for a fully developed velocity profile.

Droplet size

The droplet diameter has been varied from one-half to two times the nominal value of 0.000762 m. Only the radiation and void fraction portions of the model are affected since the droplet diameter is not included in the vapor generation source function. The variation in calculated wall superheats is less than 3°C, from the nominal droplet diameter calculations.

Strength of source function

The variation in wall and vapor superheats with the strength of the vapor generation source is depicted in Figs. 5 and 6. As the strength increases, both superheats decrease. The temperature difference, however, remains fairly constant. This small range of temperature difference indicates that the present form of the distributed heat sinks does not significantly effect the turbulent convective heat transfer. This conclusion is similar to the results of Siegel and Sparrow [34] for uniform heat sources in turbulent flow.

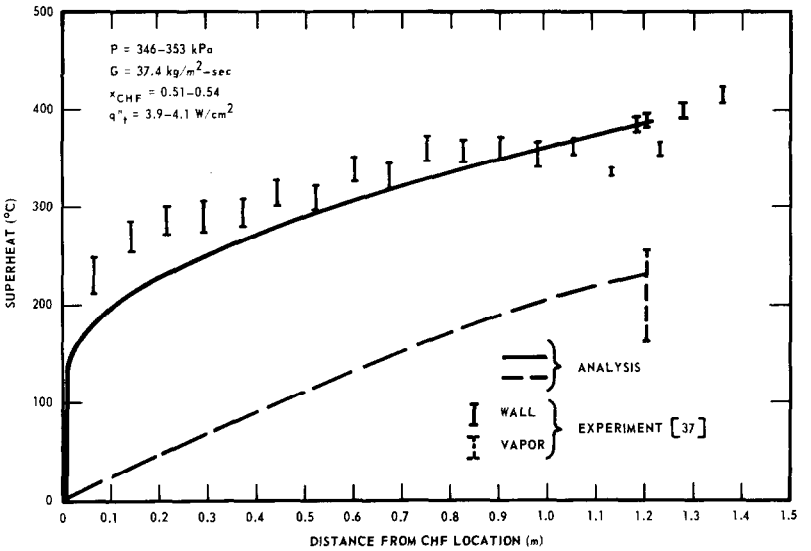

FIG. 7. Superheat temperature scatter.

Data-model comparison

As mentioned previously, experimental data on post-CHF boiling with simultaneous measurement of wall and vapor superheats are rare. The most recent steam–water data of Nijhawan [39] have been used in this evaluation. A total of 16 arbitrarily selected data points have been used encompassing the following ranges of parameters:

Pressure	234.0–373.0 kPa
Total Mass Flux	18.7–42.3 kg/m²-s
CHF Quality	0.12–0.57
Wall Heat Flux	1.3–6.5 W/cm².

Considerable data scatter for the vapor superheat measurements for essentially the same conditions has been found. Figure 7 shows the scatter band for five sets of data taken during the same run. Wall superheat variations are typically ±15°C, while the maximum variation in vapor superheat is ± 45°C. Also shown on this figure are the analytical superheat predictions. The average wall superheat was matched by the model to determine the strength of the vapor generation source function. The predicted vapor superheat is well

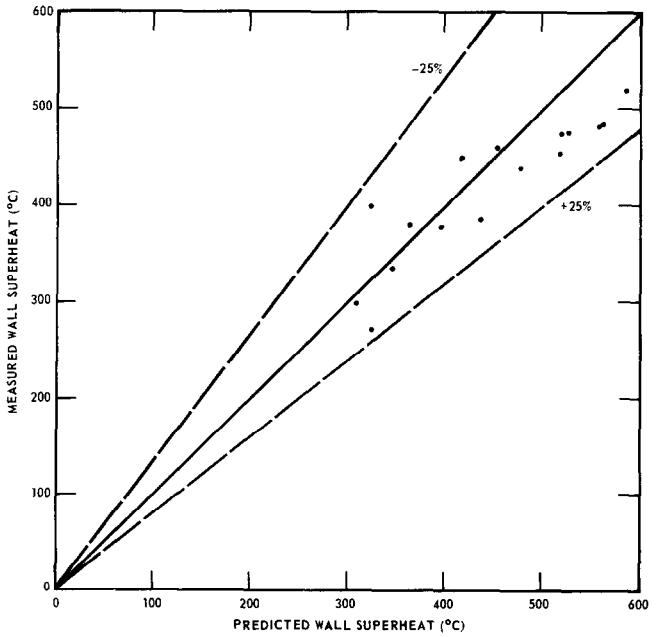

FIG. 8. Wall superheat data-model comparison.

within the maximum variation from the experiments.

The model was compared to the sixteen data points by varying the value of a for each run until the vapor temperature was matched at the measurement location. The value of a in the vapor generation source function varied from 0.0 to 1.9 kg/m^3-s-°C for these 16-data points. The predicted and measured *wall* superheats are then compared at this location as shown in Fig. 8. The average deviation of the predicted wall superheat is +6.6% with respect to the measured values. Therefore, if the value of a in the vapor generation source function can be successfully correlated to predict the correct vapor temeratures, the present model can successfully predict wall temperatures.

If desired, the wall temperature could be matched and the predicted and measured vapor superheats could also be compared as shown in Fig. 9. As expected, this average deviation for the vapor superheat is similar to the wall superheat deviation and is −7.9% with respect to the measured values. By comparison, the average deviation using a standard single-phase convective heat transfer coefficient such as calculated by the Dittus–Boelter correlation gives an average deviation of −58%. Therefore, the present model represents a distinct improvement, at least for the experimental data of Nijhawan, over using a single-phase correlation.

Model assessment

The present model predicts the wall superheat well, particularly at larger distances from the CHF location. The wall superheat discrepancy near the CHF location may be due to the uncertainty in locating the exact CHF point. The actual value could be as much as 0.10 m earlier than assumed in the calculations. The difference in the shape of the axial wall temperature curve may also be attributable to the fact that a constant value of a was used for each run in the present model. Actually, the value of a will change along the channel which will alter the predicted wall superheat profile. Work is continuing on predicting the value of a from local operating conditions.

CONCLUSIONS

(1) Consideration of vapor generation will significantly reduce the calculated wall superheat for post-CHF flow.

(2) The contribution of radiation heat transfer is small in the present case.

(3) In spite of a continually developing flow situation, a fully developed velocity profile for the vapor can be assumed.

(4) The droplet size is not important in this vapor generation source function model.

(5) The wall–vapor temperature difference is approximately constant for a given set of conditions irrespective of the strength of the vapor generation source function. Therefore, the assumed distribution of heat sinks has a small effect on the turbulent convective heat transfer at the wall.

(6) The vapor superheat data show considerable scatter for the same conditions.

(7) The average deviation of the data–model comparison is − 7.9% and + 6.6% for the vapor and wall superheats, respectively.

The vapor generation source function approach can be used to accurately describe post-CHF heat transfer. Calculated and measured wall and vapor superheats have been compared, for the first time in turbulent

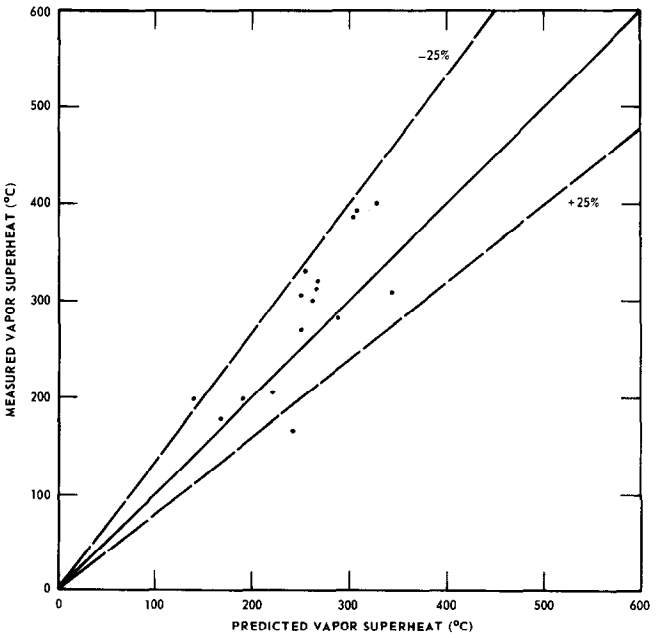

FIG. 9. Vapor superheat data-model comparison.

flow. Correlation of the variable a in the vapor generation source function with operating conditions is currently being pursued. With the correlation of a, the model will be able to predict the wall and vapor superheats in turbulent post-CHF flow-boiling of dispersed two-phase flows.

Acknowledgements—The authors wish to express their appreciation to the United States Nuclear Regulatory Commission for support during this investigation. The suggestions of Dr. Y. Y. Hsu of U.S.N.R.C. were especially appreciated.

REFERENCES

1. J. D. Parker and R. J. Grosh, Heat Transfer to a Mist Flow, ANL-6291 (1962).
2. K. H. Sun, J. M. Gonzalez-Santalo and C. L. Tien, Calculations of Combined Radiation and Convection Heat Transfer in Rod Bundles Under Emergency Cooling Conditions, *Trans. ASME, J. Heat Transfer* **98,** 414–420 (1976).
3. G. E. Dix and J. G. M. Andersen, Spray Cooling Heat Transfer for a BWR Fuel Bundle, *Symp. Thermal and Hydraulic Aspects of Nuclear Reactor Safety, Vol. 1 Light Water Reactors, ASME,* 217–248 (1977).
4. S. Yao, Convective Heat Transfer of Laminar Droplet Flow in Thermal Entrance Region of Circular Tubes, *Trans. ASME, J. Heat Transfer* **101,** 480–483 (1979).
5. A. Rane and S. Yao, Heat Transfer of Evaporating Droplet Flow in Low Pressure Systems, ASME Paper No. 79-WA/HT-10.
6. S. Yao and A. Rane, Heat Transfer of Laminar Mist Flow in Tubes, *Trans. ASME, J. Heat Transfer* **102,** 678–683 (1980).
7. S. Wong, A Model for Dispersed Flow Heat Transfer During Reflood, Ph.D. Thesis, Carnegie-Mellon University (1979).
8. S. Wong and L. E. Hochreiter, A Model for Dispersed Flow Heat Transfer During Reflood, *Experimental and Analytical Modeling of LWR Safety Experiments, ASME* 11–22 (1980).
9. S. Yao and A. Rane, Numerical Study of Turbulent Droplet Flow Heat Transfer, ASME Paper No. 80-WA/HT-48 (1980).
10. D. C. Groeneveld, Post-Dryout Heat Transfer: Physical Mechanisms and a Survey of Prediction Methods, *Nucl. Engng Design* **32,** 283–294 (1975).
11. V. H. Ransom *et al.*, RELAP5/MOD1 Code Manual Vol. I—System Models and Numerical Methods (Draft), NUREG/CR-1826 EG&G-2070 (Nov. 1980).
12. TRAC-P1: An Advanced Best Estimate Computer Program for PWR LOCA Analysis, NUREG/CR-0063, LA-7279-MS (June 1978).
13. M. Ishii, *Thermo-Fluid Theory of Two-Phase Flow,* Eyrolles, Paris (1975).
14. L. Arrieta and G. Yadigaroglu, Analytical Model for Bottom Reflooding Heat Transfer in Light Water Reactors (The UCFLOOD Code), EPRI NP-756 (Aug. 1978).
15. A. Ghazanfari, E. F. Hicken and A. Ziegler, Unsteady Dispersed Flow Heat Transfer Under Loss-of-Coolant Accident Related Conditions, *Nucl. Technol.* **51,** 21–26 (1980).
16. M. Cumo, G. E. Farello, G. Ferrari and G. Palazzi, On Two-Phase Highly Dispersed Flows, *Trans. ASME, J. Heat Transfer* **96,** 496–503 (1974).
17. S. L. Lee and F. Durst, On the Motions of Particles in Turbulent Flows, NUREG/CR-1554 (July 1980).
18. *1967 ASME Steam Tables,* 2nd edn., ASME (1967).
19. M. M. Abu-Romia and C. L. Tien, Appropriate Mean Absorption Coefficients for Infrared Radiation of Gases, *Trans. ASME, J. Heat Transfer* **89,** 321–327 (1967).
20. F. M. White, *Viscous Fluid Flow,* McGraw-Hill, New York (1974).
21. S. I. Pai, On Turbulent Jet Mixing of Two Gases at Constant Temperature, *Trans. ASME, J. appl. Mech.* **77,** 604 (1955).
22. Y. Y. Hsu and J. M. Smith, The Effect of Density Variation on Heat Transfer in the Critical Region, *Trans. ASME, J. Heat Transfer* **83,** 176–182 (1961).
23. S. Levy, Prediction of Two-Phase Pressure Drop and Density Distribution from Mixing Length Theory, *Trans. ASME, J. Heat Transfer* **85,** 137–152 (1963).
24. T. Y. Na and I. S. Habib, Heat Transfer in Turbulent Pipe Flow Based on a New Mixing Length Model, *Appl. Sci. Res.,* **28A,** 302–314 (1973).
25. J. Nikuradse, Gesetzmäbigkeit der turbulenten Strömung in Glatten Rohren, *Forsch. Arb. Ing.-Wes.* No. 356 (1932), as presented in H. Schlicting, *Boundary-Layer Theory,* 6th edn. McGraw-Hill, New York.
26. E. R. Van Driest, On Turbulent Flow Near a Wall, *J. aero. Sci.* **23,** 1007 (1956).
27. S. W. Webb, Turbulent Prandtl Numbers for Air in Wall-Bounded Shear Flow, unpublished work (1980).
28. N. Z. Azer and B. T. Chao, A Mechanism of Turbulent Heat Transfer in Liquid Metals, *Int. J. Heat Mass Transfer* **1,** 121–138 (1960).
29. H. B. Keller, Numerical Methods in Boundary-Layer Theory, *Ann. Rev. Fluid Mech.* **10,** 417 (1978).
30. R. D. Ackerberg and J. H. Phillips, The Unsteady Laminar Boundary Layer on a Semi-Infinite Flat Plate Due to Small Fluctuations in the Magnitude of the Free Stream Velocity, *J. Fluid Mech.* **51,** 137–157 (1972).
31. W. F. Ames, *Numerical Methods for Partial Differential Equations,* 2nd edn. Academic Press (1977).
32. E. M. Sparrow and R. Siegel, Laminar Tube Flow with Arbitrary Internal Heat Sources and Wall Heat Transfer, *Nucl. Sci. Engng* **4,** 239–254 (1958).
33. E. M. Sparrow, T. M. Hallman and R. Siegel, Turbulent Heat Transfer in the Thermal Entrance Region of a Pipe with Uniform Heat Flux, *Appl. Sci. Res.* **7A,** 37–52 (1957).
34. R. Siegel and E. M. Sparrow, Turbulent Flow in a Circular Tube with Arbitrary Internal Heat Sources and Wall Heat Transfer, *Trans. ASME, J. Heat Transfer* **81,** 280–290 (1959).
35. R. E. Mueller, Film Boiling Heat Transfer Measurements in a Tubular Test Section, EURAEC-1971/GEAP-5423 (1967).
36. E. E. Polomik, Transition Boiling Heat Transfer Program—Final Summary Report for Feb/63-Oct/67, GEAP-5563, (Oct. 1967).
37. L. E. Hochreiter, NRC/Westinghouse/EPRI FLECHT Low Flooding Rate Skew Axial Profile Results, Presented at the 5th Water Reactor Safety Information Meeting, sponsored by U.S.N.R.C., Washington, D.C. (1977).
38. S. Nijhawan, J. C. Chen, R. K. Sundaram and E. J. London, Measurement of Vapor Superheat in Post-Critical-Heat-Flux Boiling, *Trans. ASME, J. Heat Transfer* **102,** 465–470 (1980).
39. S. Nijhawan, Experimental Investigation of Thermal Non-Equilibrium in Post-Dryout Steam–Water Flow, Ph.D. Dissertation, Lehigh University (1980).
40. S. M. Nijhawan, J. C. Chen and R. K. Sundaram, Parametric Effects on Vapor Nonequilibrium in Post-Dryout Heat Transfer, ASME Paper No. 80-WA/HT-50 (1980).
41. S. W. Webb and J. C. Chen, A Non-Equilibrium Model for Post-CHF Heat Transfer, *Proc. OECD (NEA) CSNI Third Spec. Meet. on Trans. Two-Phase Flow: Pasadena, Calif.* CSNI Report No. 61. (March 1981).
42. D. C. Slaughterbeck, W. E. Vesely, L. J. Ybarrondo, K. G. Condie and R. J. Mattson, Statistical Regression Analysis

of Experimental Data for Flow Film Boiling Heat Transfer, ASME Paper No. 73-HT-20 (1973).
43. L. S. Tong and J. D. Young, A Phenomenological Transition and Film Boiling Heat Transfer Correlation, *Proc. 5th Int. Heat Transfer Conf., Tokyo*, Vol. IV, paper B 3.9 (1974).
44. D. C. Groeneveld and G. G. J. Delorme, Prediction of Thermal Non-Equilibrium in the Post-Dryout Regime, *Nucl. Engng. Design* **36**, 17–26 (1976).
45. W. F. Laverty and W. M. Rohsenow, Film Boiling of Saturated Nitrogen Flowing in a Vertical Tube, *Trans. ASME, J. Heat Transfer* **89**, 90–98 (1967).
46. R. P. Forslund and W. M. Rohsenow, Dispersed Flow Film Boiling, *Trans. ASME, J. Heat Transfer* **80**, 399–407 (1968).
47. S. J. Hynek, W. M. Rohsenow and A. E. Bergles, Forced Convection Dispersed Flow Film Boiling, MIT Heat Transfer Laboratory Report No. DSR 70586-63 (1969). (1969).
48. O. C. Iloeje, D. N. Plummer, W. M. Rohsenow and P. Griffith, A Study of Wall Rewet and Heat Transfer in Dispersed Vertical Flow, MIT Heat Transfer Laboratory Report No. 72718-92 (1974).
49. D. N. Plummer, P. Griffith and W. M. Rohsenow, Post-Critical Heat Transfer to Flowing Liquid in a Vertical Tube, Paper No. 76-CSME/CSChE-13, 16th National Heat Transfer Conference, St. Louis (1976).
50. J. C. Chen, R. K. Sundaram and F. T. Ozkaynak, A Phenomenological Correlation for Post-CHF Heat Transfer, U.S.N.R.C. Report NUREG-0237 (June 1977).
51. E. N. Ganic and W. M. Rohsenow, Dispersed Flow Heat Transfer, *Int. J. Heat Mass Transfer* **20**, 855–866 (1977).
52. O. C. Jones and N. Zuber, Post-CHF Heat Transfer: A Non-Equilibrium, Relaxation Model, *17th National Heat Transfer Conference, Salt Lake City* (1977).
53. P. Saha, B. S. Shiralkar and G. E. Dix, A Post-Dryout Heat Transfer Model Based on Actual Vapor Generation Rate in Dispersed Droplet Regime, ASME Paper No. 77-HT-80 (1977).

UN MODELE NUMERIQUE DU TRANSFERT THERMIQUE POUR UN ECOULEMENT TURBULENT ET UNE PHASE DISPERSEE ET HORS D'EQUILIBRE

Résumé—Un modèle analytique est développé pour décrire le transfert thermique pour un écoulement déphasique avec une phase dispersée et hors d'équilibre après la crise d'ébullition (CHF). L'absence d'équilibre thermodynamique est traitée à travers une fonction source de génération de vapeur dans les équations pour représenter l'effet de puits de chaleur et de source de masse lors de l'évaporation des gouttelettes. On évalue les effets des différents composants du modèle. Une comparaison limitée entre le modèle et les données expérimentales montre les écarts moyens de $-7{,}9$ et $+6{,}6\%$ pour la vapeur et pour la surchauffe de la paroi.

EIN NUMERISCHES MODELL FÜR DEN WÄRMEÜBERGANG IN TURBULENTEN DISPERSEN NICHTGLEICHGEWICHTSSTRÖMUNGEN

Zusammenfassung—Es wurde ein analytisches Modell zur Beschreibung des Wärmeübergangs in zweiphasigen turbulenten dispersen Nichtgleichgewichtsströmungen beim Strömungssieden im Bereich der überkritischen Wärmestromdichte entwickelt. Das thermodynamische Nichtgleichgewicht wird mit einer Quellfunktion für die Dampferzeugung in den Erhaltungsgleichungen des Dampfes behandelt, um den Wärmesenken- bzw. Stoffquellen-Effekt der Tröpfchenverdampfung wiederzugeben. Die Einflüsse der verschiedenen Komponenten werden im Modell abgeschätzt. Ein begrenzter Vergleich zwischen Experiment und Rechenmodell zeigt in Bezug auf die gemessenen Werte mittlere Abweichungen von $-7{,}9$ und $+6{,}6$ Prozent für die berechneten Dampf- und Wandüberhitzungen.

ЧИСЛЕННАЯ МОДЕЛЬ ТЕПЛОПЕРЕНОСА ПРИ ТУРБУЛЕНТНОМ НЕРАВНОВЕСНОМ ДИСПЕРСНОМ ТЕЧЕНИИ

Аннотация — Предложена аналитическая модель для расчета переноса тепла при двухфазном турбулентном неравновесном дисперсном течении в закризисной области кипения. Термодинамически неравновесное состояние анализируется с помощью функции источника парообразования, введенной в уравнения сохранения пара, что позволяет учесть влияние стока тепла/источника массы при испарении капель. Модель учитывает влияние различных параметров. Сравнение расчета по модели, учитывающей влияние ограниченного числа параметров, с экспериментом дает расхождение для значений перегрева пара и стенки, равных соответственно $-7{,}9\%$ и $+6{,}6\%$.